Pharm Res (2012) 29:1255–1269
DOI 10.1007/s11095-011-0660-x

RESEARCH PAPER

Optimization of Magnetic Nanoparticle-Assisted Lentiviral Gene Transfer

Christina Trueck • Katrin Zimmermann • Olga Mykhaylyk • Martina Anton • Sarah Vosen • Daniela Wenzel • Bernd K. Fleischmann • Alexander Pfeifer

Received: 3 August 2011 / Accepted: 19 December 2011 / Published online: 25 January 2012

ABSTRACT

Purpose Targeting of specific cells and tissues is of great interest for clinical relevant gene- and cell-based therapies. We use magnetic nanoparticles (MNPs) with a ferrimagnetic core (Fe_3O_4) with different coatings to optimize MNP-assisted lentiviral gene transfer with focus on different endothelial cell lines.

Methods Lentiviral vector (LV)/MNP binding was characterized for various MNPs by different methods (e.g. magnetic responsiveness measurement). Transduced cells were analyzed by flow cytometry, fluorescence microscopy and iron recovery. Cell transduction and cell positioning under physiological flow conditions were performed using different *in vitro* and *ex vivo* systems.

Results Analysis of diverse MNPs with different coatings resulted in identification of nanoparticles with improved LV association and enhanced transduction properties of complexes in several endothelial cell lines. The magnetic moments of LV/MNP complexes are high enough to achieve local gene targeting of perfused endothelial cells. Perfusion of a mouse aorta with LV/MNP transduced cells under clinically relevant flow conditions led to local cell attachment at the intima of the vessel.

Conclusion MNP-guided lentiviral transduction of endothelial cells can be significantly enhanced and localized by using optimized MNPs.

KEY WORDS gene targeting · lentiviral vectors · local cell positioning · magnetic nanoparticles · transduction

ABBREVIATIONS

bPAEC	bovine pulmonary arterial endothelial cell
CMV	cytomegalovirus
DMEM	Dulbecco's modified eagle's medium

Christina Trueck and Katrin Zimmermann contributed equally.

Electronic supplementary material The online version of this article (doi:10.1007/s11095-011-0660-x) contains supplementary material, which is available to authorized users.

C. Trueck • K. Zimmermann • A. Pfeifer (✉)
Institute of Pharmacology and Toxicology, Biomedical Center
University of Bonn
Sigmund-Freud-Strasse 25
53105 Bonn, Germany
e-mail: Alexander.Pfeifer@uni-bonn.de

C. Trueck • K. Zimmermann • B. K. Fleischmann • A. Pfeifer
NRW International Graduate Research School BIOTECH-PHARMA
Bonn, Germany

O. Mykhaylyk • M. Anton
Institute of Experimental Oncology and Therapy Research
Klinikum rechts der Isar der Technischen Universität München
Ismaninger Strasse 22
81675 Munich, Germany

S. Vosen • D. Wenzel • B. K. Fleischmann
Institute of Physiology I, University of Bonn
Sigmund-Freud-Strasse 25
53105 Bonn, Germany

B. K. Fleischmann • A. Pfeifer
PharmaCenter Bonn, University of Bonn
Bonn, Germany

DMF	dimethylformamide
DMSO	dimethyl sulfoxide
eGFP	enhanced green fluorescent protein
EPC	endothelial progenitor cell
FCS	fetal calf serum
FSA	lithium 3-[2-(perfluoroalkyl)ethylthio] propionate
HBSS	Hank's balanced salt solution
HBSS++	Hank's balanced salt solution + $MgCl_2$ and $CaCl_2$
hlEPC	human late endothelial progenitor cell
HUVEC	human umbilical vein endothelial cell
IP	infectious particles
LDH	lactate dehydrogenase
LV	lentiviral vector
meEPC	murine embryonal endothelial progenitor cell
MNP	magnetic nanoparticle
MOI	multiplicity of infection
MTT	3-(4,5-dimethylthiazol-2-yl)-2, 5-diphenyl-tetrazoliumbromid
PALD	palmitoyldextrane
PB	polybrene
PBS	phosphate buffered saline
PEI	polyethylenimine
PFA	paraformaldehyde
RT	reverse transcriptase
SDS	sodium dodecyl sulfate
SO	silicon oxide
SiOx/Phosphonate	silicon oxide layer with surface phosphonate groups
V'30	LV transduction without MNPs for 30 min
V'ON	LV transduction without MNPs overnight
VP	viral particles
VSV.G	glycoprotein of vesicular stomatitis virus

INTRODUCTION

Targeting of specific cells and tissues are of great importance for successful gene- and cell-based therapies. Much effort has been put in the development of strategies for guiding viral or nonviral vectors to defined body areas to efficiently introduce therapeutic genes to the target tissue. Lentiviral vectors (LVs) are powerful vehicles for gene delivery as they are able to transduce dividing and non-dividing cells (1–3). Lentiviruses belong to the large family of *Retroviridae* and can stably integrate their genetic information into the host genome (4–6), which is necessary for persisting gene expression. Importantly, LVs have already been used in first clinical gene therapy trials (e. g. (7,8)). In order to achieve local lentiviral gene transfer different approaches have been developed, including various pseudotypization of the viral vectors as well as application of cell- or tissue specific promoters to drive the transgene expression (9). However, use of cell-specific promoters does not provide local specificity of gene transfer. Targeted regional virus infection can be achieved by binding of viral vectors to magnetic nanoparticles (MNPs) and local application of a magnetic gradient field (10,11).

MNPs can also form complexes with nucleic acids or chemotherapeutic agents (10,12). A century ago, Paul Ehrlich already postulated the creation of "magic bullets" for use in targeting of drugs to specific locations in the human body (13). MNP-based drug delivery can increase the efficiency and specificity of drugs. Therefore, a much smaller dose would be administered systemically and unwanted side effects could be reduced, which is especially important for chemotherapeutic drugs and their high toxicity. In combination with magnetizable stents drug coupled MNPs were already successfully applied for local drug delivery (14) as well as MNP loaded endothelial cells for local cell positioning (15).

Here, we optimized the association of VSV.G pseudotyped LVs to MNPs that have a ferrimagnetic magnetite core (Fe_3O_4) and differ in their coating layer, composition, hydrodynamic diameter and surface charge. We screened various MNPs to achieve magnetically guided high transduction efficiency in different endothelial cells. Using an optimal combination of LV/MNP complexes under physiological flow conditions leads to highly efficient local gene targeting of endothelial cells at the site of magnetic gradient field application. Additionally, cells transduced with LV/MNP complexes are magnetically labeled and can thus be trapped in a magnetic gradient field.

MATERIALS AND METHODS

Cell Culture Conditions

HUVECs (Human Umbilical Vein Endothelial Cells) and bPAECs (bovine Pulmonary Arterial Endothelial Cells) (both Provitro, Berlin, Germany) were cultured in Endothelial Cell Growth Medium (C-22010; Promocell, Heidelberg, Germany) at 5% CO_2 and 37°C. Cells were frozen at early passages.

hlEPCs (human late Endothelial Progenitor Cells (EPCs)) were isolated by Ulrich Becher (University of Bonn, Germany) from human blood as described below according to

regulations by the Institutional Review Board at the University Hospital of Bonn. In detail, mononuclear cells from blood of healthy volunteers were obtained by density gradient centrifugation with Ficoll-Paque Plus (Amersham Biosciences, GE Healthscare, Uppsala, Sweden). Isolated mononuclear cells were plated at a density of 2E+07 cells per well on 6well plates coated with human fibronectin (R&D Systems, Minneapolis, MN, US) in endothelial cell basal medium-2 (EBM-2) with 5% fetal calf serum (FCS) and growth factors (Lonza, Basel, Switzerland). Early colonies appeared at around two to three weeks. At 4 weeks, subconfluent cell colonies were passaged and master stocks were established (=late EPCs). Cells were cultivated in supplemented EBM-2 at 5% CO_2 at 37°C.

Murine embryonal EPCs (meEPCs) were a kind gift of Christian Kupatt (LMU Munich, Germany) and originally isolated by Hatzopoulos *et al.* (16). Cultivation of meEPCs was performed in Dulbecco's Modified Eagle's Medium (DMEM, Invitrogen, Darmstadt, Germany) supplemented with 20% FCS, 5% Pen/Strep (both Biochrom, Berlin, Germany) and 5% non essential amino acids (Invitrogen, Darmstadt, Germany) and cultured at 5% CO_2 at 37°C.

Production of LVs

A self-inactivating lentivector (rrl-CMV-eGFP) containing a CMV-driven eGFP expression cassette (17) was used. Preparation and purification of LVs was accomplished as already described (18). Briefly, the producer cells (human embryonal kidney cells, HEK293T) were transfected with the lentivector and packaging plasmids (19). Medium was changed on the next day and the cell culture supernatant was harvested 24 h and 48 h after the addition of fresh medium. Cell debris was removed by using a bottle-top filter (SFCA, 0.45 µm, Nalgene, Thermo Fisher Scientific, Waltham, MA, USA). Purification was performed by ultracentrifugation and the LV pellets were finally resuspended in HBSS (Hank's balanced salt solution, Invitrogen, Darmstadt, Germany).

Titration of LVs

To determine the biological titer (in infectious particles (IP)/ml) of the LV preparation, HEK293T cells were seeded in a 24well plate (Sarstedt, Nuembrecht, Germany), transduced with virus of serial dilutions and analyzed using flow cytometry as already described (18). The physical titer was measured by use of a colorimetric reverse transcriptase assay (Roche Diagnostics, Indianapolis, IN, USA) quantifying active reverse transcriptase (RT). Considering average amount of molecules per viral particle, molecular weight and Avogadro constant, the following term was used for calculating the viral particles per ml (VP/ml): VP/ml = ng RT/µl x 1E-09/3.88E-19.

Synthesis and Characterization of MNPs

Core-shell type iron oxide MNPs were synthesized by precipitation of Fe(II)/Fe(III) hydroxide from aqueous solution of a mixture of Fe(II) and Fe(III) salts, followed by transformation into magnetite in an oxygen-free atmosphere with spontaneous adsorption or condensation of shell components as described elsewhere (20–22). To modify the surface of the MNPs PEI-Mag2 and PEI-Mag3, the fluorinated surfactant ZONYL FSA (lithium 3-[2-(perfluoroalkyl)ethylthio]propionate) was combined with 25-kDa branched polyethylenimine (PEI) in ratios of 68 and 32% (w/w) for PEI-Mag2 or 6 and 94% (w/w) for PEI-Mag3 (23). For SO-Mag1 and SO-Mag5 nanoparticles, the surface coating was formed by condensation of tetraethyl orthosilicate and 3-(trihydroxysilyl)propylmethylphosphonate resulting in a silicon oxide layer with surface phosphonate groups (SiOx/Phosphonate). Decoration of the surface of SO-Mag1 particles with PEI at a PEI-to-iron ratio of 5% (w/w) resulted in SO-Mag2 particles with SiOx/Phosphonate-PEI coating (21). The particles synthesized in the presence of the fluorinated surfactant ZONYL FSE with cationic polymer hexadimethrine bromide (polybrene; PB) are referred to as PB-Mag1 nanoparticles and those synthesized using a combination of the ZONYL FSA with PB are denoted as PB-Mag2 MNPs. To modify the surface of the magnetite nanoparticles PALD1-Mag4 and PALD2-Mag1 the fluorinated surfactant ZONYL FSE was combined with palmitoyl dextran PALD1 and PALD2, respectively. Palmitoyl dextran PALD1 and PALD2 with 11 and 32 palmitoyl groups per 100 dextran units were synthesized by means of esterification of Dextran-10 (Amersham Biosciences, GE Healthscare, Uppsala, Sweden) with palmitoyl chloride (Sigma Aldrich, Munich, Germany) as described previously (24).

The resulting coated MNPs suspensions were dialyzed against double distilled water to remove unbound coating components and then sterilized using ^{60}Co gamma-irradiation with a dosage of 25 kGy (25). The particle stock concentrations in terms of dry weight and iron content were determined as described previously (20). Average crystallite size $\langle d \rangle$ of the core was calculated from the X-ray diffraction data using the Scherer formula (26). Mean hydrodynamic diameter (D_h) and electrokinetic (ξ) potential of the MNPs suspended in double distilled water were measured by photon correlation spectroscopy using a Malvern 3000 HS Zetasizer (Malvern, Herrenberg, Germany). The saturation magnetization per unit of iron weight (M_s) was measured at 298 K using a vibrating sample magnetometer (Oxford Instruments, Oxfordshire, UK.).

LV/MNP Assembling

LVs and MNPs were incubated in 300 µl HBSS supplied with $MgCl_2$ and $CaCl_2$ (HBSS++; Invitrogen, Darmstadt,

Germany) at room temperature for 20 min. Beside HBSS++ also other solutions were tested for the assembling of nanoparticles with LVs: 0.9% (w/v) NaCl, 0.01 M NaCl, H_2O or FCS. Furthermore, LV/MNP complexes were formed in HBSS++ as described above and subsequently the same volume serum (50% (w/v)) was added to the preformed complexes. The suspensions were then transferred to a 24well plate (without cells). After incubation for 30 min at 4°C on a magnetic plate (chemicell, Berlin, Germany), the supernatant (= not magnetically sedimented, uncomplexed LVs) was used for an ELISA detecting the lentiviral capsid protein p24 according to the manufacturer's instructions (RETRO-TEK HIV-1 p24 Antigen ELISA, Zeptrometrix Corporation Buffalo, NY, USA). As reference LV suspension without MNPs was used.

Different LV/MNP ratios between 1 and 1,000 fg Fe/VP were analyzed with increasing MNP concentration (mg Fe/ml) and a fixed concentration of VPs (ca. 4E+06 VP/ml). VP concentrations were calculated by measuring the physical titer of the LV preparation (as described above), because complexation of MNPs also occurs with biologically inactive particles that are not measured with the biological titer.

LV/MNP Cell Transduction

Cells were seeded on 24-, 6well (BD Falcon, Franklin Lakes, NJ, USA) or 12well (Greiner Bio one, Frickenhausen, Germany) cell culture plates. The volume of LV preparation needed for transduction (calculated from the biological LV titer) was adjusted to the desired MOI (multiplicity of infection, MOI 5). The viral particles (physical titer) in the volume applied were determined and according to desired LV/MNP ratio (fg Fe/VP) and the MNP iron concentration the volume of the MNP suspension was calculated. LVs and MNPs were incubated in 300 µl to 800 µl HBSS++ for 20 min.

For transduction the cells were incubated with the LV/MNP suspension for 30 min at 4°C on a magnetic plate (chemicell, Berlin, Germany). Afterwards the LV/MNP solution was replaced with cell culture medium. Buffer without LVs and MNPs or with LV but without MNPs was used as control as well as transduction with LV without MNPs, but overnight at 37°C at 5% CO_2 (in medium). Cells were incubated for 48 h.

Magnetic Responsiveness Measurements

Magnetic responsiveness of LV/MNP complexes or LV/MNP transduced and magnetically labeled cells was determined as described previously (24,27). The method is based on measuring the turbidity of the LV/MNP complexes/cell suspensions upon application of a magnetic gradient field. Briefly, 500 µl aliquots of the cells/complexes suspension were put into an optical cuvette positioned in the holder, transferred to a spectrophotometer (Beckman DU 640, Beckman Coulter Incorporated, Brea, CA, USA) and exposed to a defined magnetic gradient field. The time course of turbidity at 300 nm was then recorded as a function of time. The magnetic gradient field was generated by positioning two mutually attracting packs of four quadrangular neodymium-iron-boron (Nd-Fe-B) permanent magnets (17×17×4 mm) in symmetric fashion on each side of the cuvette holder and parallel to the light beam. The resulting magnetic gradient field was measured in a 1-mm grid in planes at different distances from the surface of the Nd-Fe-B magnet packs using a Hall probe. The z-component of the field gradient perpendicular to the surface of the magnets was calculated. In the measuring window, the magnetic gradient field was rather uniform in the X-Y plane parallel to both the surface of the magnets and the light beam with an average magnetic induction $< B >$ and a field gradient $<\nabla B>$, both perpendicular to the light beam, of 213 mT and 4 Tm^{-1}, respectively. The recorded optical densities were normalized to the data at t=0. The experimental clearance curves were well fitted to a single exponential decay curve ($y = A_1\exp(-x/t_1)$), using OriginPro8 Data Analysis Software, and the time required for the 10 fold decrease of the optical density was calculated as $t_{0.1} = t_1 \ln$ (10). The magnetophoretic mobility was calculated as $v_z=\langle L\rangle/t_{0.1}$. Here, $\langle L\rangle$=1 mm is the average path of the complexes' movement perpendicular to the measuring light beam symmetrically in both directions to the magnets arranged at both sides of the optical cuvette (4 mm wide). The average magnetic moment (M) of the complexes can then be calculated with account for the average hydrodynamic diameter and characteristics of the magnetic core of the MNPs as previously described (24). LV/MNP suspensions contained 7.2 µg Fe and 2.4E + 07 VPs in 240 µl HBSS++ (assembling for 20 min) and were diluted 10 fold before measurements. Approximately 1E + 05 LV/MNP transduced cells were PFA fixed (48 h after transduction) and resuspended in 550 µl HBSS++ for analysis.

Hydrodynamic Diameter and Electrokinetic Potential of LV/MNP Complexes

The hydrodynamic diameter (D_h) and electrokinetic potential (ξ) of LV/MNP complexes were measured in HBSS++ at a final virus concentration of 1E+07 VP/ml by photon correlation spectroscopy using the Zetasizer Nano ZS (Malvern, Herrenberg, Germany).

Analysis of Transgene Expression

Images of cells were taken 48 h after LV (+/- MNP) transduction with an inverted microscope DMIL 4000 (Leica Microsystems, Wetzlar, Germany) equipped with a GFP

fluorescence filter. LV transduced cells (with or without MNPs) were also analyzed by flow cytometry. These cells were fixed 48 h after transduction with 4% (w/v) PFA (15 min, 4°C) and resuspended in PBS. FACS analysis of the cells was performed using the Coulter epics XL-MCL flow cytometer (Beckman Coulter Incorporated, Brea, CA, USA) and evaluated using WinMDI2.8 software.

Toxicity Assays of Transduced Cells

Potential toxicity was evaluated either by using LDH (lactate dehydrogenase) or MTT assay: Briefly, 20,000 cells were seeded in a 24well plate and transduced with LV/MNP complexes (or LV alone) as described above. After approximately 18 h the cell culture supernatant was centrifuged to pellet cell debris and supernatant was analyzed using the LDH assay according to the manufacturer's instruction (Cytotoxicity Detection kit plus, Roche Diagnostics, Indianapolis, IN, USA). For the MTT assay, 10 µl of a 0.5% (w/v) 3(4,5-Dimethylthiazol-2-yl)-2,5-diphenyl-tetrazoliumbromid (MTT) solution was added to the transduced cells (ca. 18 h after transduction). Cells were incubated for 2 h at 37°C. Cell culture supernatant was then removed and cells were lysed by addition of an acidic SDS/DMF solution. After shaking for 15 min in the dark they were subsequently incubated at 37°C for 30 min. The suspension was transferred to a 96well plate and optical density was measured at 540 nm (reference wavelength: 620 nm).

Non-Heme-Iron Assay of Transduced Cells

Cells were transduced with LV/MNP complexes as described above. 48 h after transduction cells were centrifuged (289×g, 5 min) and cell pellet was frozen at -80°C. Cells were lysed by adding an acid mixture containing 3 M HCl and 0.6 M trichloracetic acid overnight at 65°C and analyzed for non-heme iron content using 1,10-phenantroline method as previously described (28). For preparing a calibration curve ammoniumferrum(II)sulfate monohydrate was used as standard and procedure was performed accordingly but without addition of the acid mix.

LV/MNP Cell Transduction Under Flow Conditions

3E+05 HUVECs were seeded in a µ-Slide I 0.4 Luer ibiTreat flow chamber (ibidi, Martinsried, Germany) according to the manufacturer's instructions. 48 h later LV/MNP complexes were formed in HBSS++ as described above. The flow system without the culture slide attached was equilibrated with 11.2 ml culture medium for 5 min and the virus complex solution was added and mixed by circulation for 5 min. Subsequently the flow chamber, seeded with HUVECs was attached and circulation proceeded for 15 min at 5 ml/min with an ibidi pump system (ibidi, Martinsried, Germany; shear stress 6.58 dyn/cm^3, shear rate 658 s^{-1}) with or without positioning of three permanent Nd-Fe-B magnets (Nd-Fe-B Neodelta with 1080–1150 mT; d=6 mm, h=5 mm (IBS Magnet, Berlin, Germany)), placed in a row in a holder for 96 well magnets in strictly alternating polarization. After perfusion, cells were washed 5 times with medium without application of a magnetic gradient field and fluorescence images were taken using an AxioVert 135 microscope (Zeiss, Jena, Germany). 48 h later cells were detached and seeded on cell culture dishes for cell expansion. Quantitative analysis of transgene expression was performed by flow cytometry.

Ex Vivo Flow Loop Perfusion of Murine Aorta

100,000 LV/MNP transduced HUVECs were collected in 800 µl medium 48 h after transduction. For additional loading of cells with MNPs, 100 pg Fe SO-Mag5 per seeded cell (in HBSS++) was applied to the cells for 30 min on a magnetic plate prior (around 12 h) to LV/MNP transduction.

An explanted murine aorta was connected to two cannulas and perfused *ex vivo* with 12 ml DMEM medium (Invitrogen, Darmstadt, Germany) (11). Two cylindrical (5 mm diameter, 14 mm height) Nd-Fe-B magnets were placed as close as possible to the aorta. Cells were added to the medium and the aorta was perfused for 30 min with a peristaltic pump at a flow rate of 4 ml/min. The vessel was PFA fixed and embedded in Tissue-Tek O.C.T. (Sakura, Zoeterwoude, NL). Cryosections were made and analyzed by fluorescence imaging.

Statistics

For statistical analysis the program GraphPad Prism5 was used. Statistical significance was determined by one-way analysis of variance (ANOVA) and Dunnett post-hoc test. We considered $p<0.05$ as statistically significant.

One-way ANOVA (and related nonparametric tests) compare three or more groups when the data are categorized in one way. For comparing three or more groups, it is possible to pick a post test to compare pairs of group means. The Dunnett test compares all columns vs. control column.

RESULTS

Assembling of MNPs and LVs

In initial experiments we screened a broad spectrum of MNPs of the core-shell type that differ concerning their coating, size and surface charge (Supplementary Table S1). The MNPs were bound to LVs in a physiological salt buffer supplied with $MgCl_2$ and $CaCl_2$ (HBSS++) and transduction efficiency at MOI of 5 was analyzed in

HUVECs (Human Umbilical Vein Endothelial Cells) (Supplementary Fig. S1). For further experiments, we focused on two positively charged, polyethylenimine (PEI)-coated MNPs (PEI-Mag2 and PEI-Mag3) that showed the highest transduction efficacy in HUVECs (Supplementary Fig. S1).

From the negatively charged particles, we chose two with different coatings: one with palmitoyldextran coating (PALD2-Mag1) and one carrying a silicon oxide coating with surface phosphonate groups (SO-Mag5) (Supplementary Table S1).

To identify the optimal MNP-to-LV ratio for complex formation, we assembled MNPs with LVs at increasing ratios of 1 to 1,000 fg Fe/VP and a fixed lentivirus particle concentration (Fig. 1a). Virus particle-MNP association was assessed by using an ELISA for the lentiviral capsid protein p24 in the supernatant after magnetic sedimentation of the MNP-virus complexes. The resulting dose–response curves (Fig. 1a) show increasing binding of LVs with ascending MNP concentrations for both negatively and positively charged MNPs. The plateau of the binding curve – representing the maximal assembling of LV/MNP complexes - was reached between 100 and 300 fg Fe (MNP) per VP for all particles. The amount of MNPs required for half maximal binding of LVs (Fig. 1b), was clearly higher for the negatively (PALD2-Mag1 and SO-Mag5) charged MNPs.

We used HBSS++ as buffer (containing $MgCl_2$ and $CaCl_2$), because it was previously shown that divalent cations are necessary for the complex formation of negatively charged MNPs that have the same charge as the LVs (29). Additionally, we tested the influence of different solutions on

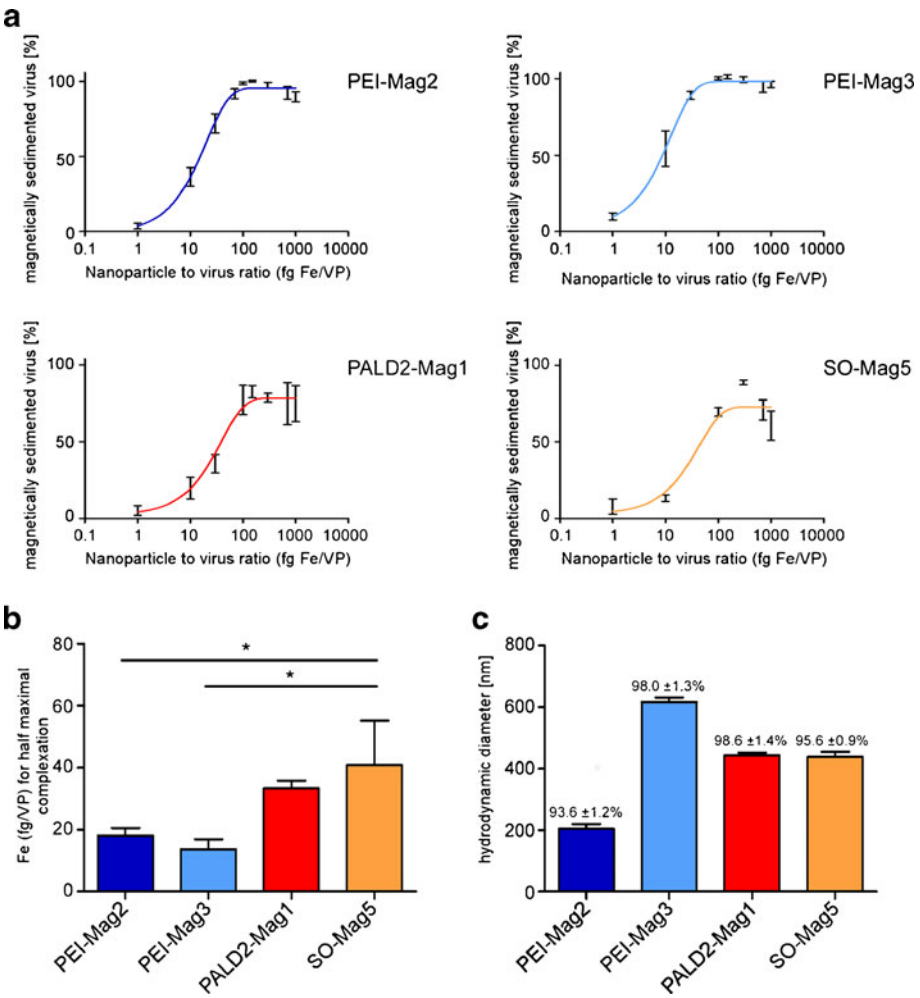

Fig. 1 Analysis of LV/MNP complexes. (**a**) Dose–response curve for cell-free LV/MNP assembly. LVs and different concentrations of MNPs (1 to 1,000 fg Fe per VP) were incubated for 20 min, transferred to 24well plate in a magnetic gradient field and supernatant (=uncomplexed virus) was analyzed using p24 ELISA. As positive control LV without MNPs was used and the percentage of complexed virus was calculated. $n \geq 3$, *mean ± SEM*. (**b**) Analysis of half maximal LV/MNP assembling. The MNP concentration per VP is displayed for different MNPs where the half of the VPs are complexed to the MNP (data is based on Fig. 1a) *($n \geq 3$, +SEM, Statistical significance compared to SO-Mag5 (calculated one-way ANOVA and post test) marked by asterisk *, $p < 0.05$)*. (**c**) Size distribution of LV/MNP complexes. LV/MNP complexes (300 fg Fe per VP) were formed in HBSS++ and the hydrodynamic diameter was measured. Of the two peaks measured for hydrodynamic diameter, only the respective main peak is displayed. On top of the bar the percentage of complexes displaying this diameter is shown. *($n=3$, +SEM)*.

MNP binding to LVs for one positively (PEI-Mag2) and one negatively (PALD-2Mag1) charged MNP (Supplementary Fig. S2a and b). Complex formation after incubation for 20 min and subsequent positioning in a magnetic gradient field for 30 min in 0.15 M (0.9% (w/v)) NaCl and HBSS++ was most efficient, whereas no assembly was detectable in H_2O or 0.01 M NaCl (apparently due to the low osmotic pressure; data not shown). Direct incubation of LVs and MNPs in FCS (serum) resulted in no detectable complex formation (Supplementary Fig. S2). However, initial LV binding to MNPs in HBSS++ followed by dilution with FCS resulted in the formation of LV/MNP complexes. At ratios above 300 fg Fe/VP, no significant difference between control (HBSS++) and HBSS++/serum condition was observed. The stability in serum is an important prerequisite for *in vivo* applications.

Another critical aspect for *in vivo* applications is the size of the LV/MNP aggregates. Therefore, we analyzed the hydrodynamic diameter of LV/MNP complexes (Fig. 1c). For all selected complexes formed in HBSS++ at a ratio of 300 fg Fe/VP two major size components were detected: the vast majority of complexes (94–99%) had a hydrodynamic diameter of around 200–600 nm (Fig. 1c) and approximately 4% of the complexes showed a larger diameter of 2.5 ± 0.1 µm (data not shown). For the LV particles suspended in HBSS++ without MNPs, we measured an average hydrodynamic diameter of 158 ± 18 nm (97.6 ± 0.6%). Thus, regarding their size, the LV/MNP complexes should be suitable for applications in small vessels that have typically a diameter of 7 µm (30). For LV/MNP assembling the final LV concentration in the suspension has no influence on the diameter of the aggregates (measured in the range of 5E+06 to 1E+09 VP/ml; data not shown).

MNP-Guided Cell Transduction

We tested magnetically guided lentiviral transduction efficiency of the LV/MNP complexes with four different MNPs (PEI-Mag2, PEI-Mag3, PALD2-Mag1, SO-Mag5) in a broad spectrum of endothelial (HUVECs and bPAECs (bovine Pulmonary Arterial Endothelial Cells)) and endothelial precursor cells (meEPCs and hlEPCs; murine embryonal Endothelial Progenitor Cells (EPCs), human late EPCs) from different species.

Lentiviral transduction requires adsorption of the viral particles to the cells before viral entry (31). Therefore, a close contact between the virus and the cells is necessary and this occurs via the Brownian motion. Brownian motion in turn is sensitive to low temperature and short incubation time and therefore the adsorption is reduced under these conditions (11,32). Association of LVs with MNPs and application of magnetic forces accelerates virus adsorption. To identify the most favorable LV/MNP transduction times, HUVECs were incubated with LV/MNP complexes for up to 60 min under application of a magnetic gradient field (Supplementary Fig. S3). The maximal transduction efficiency was achieved at approximately 20 min incubation.

First, we tested the optimal MNP-to-virus ratio in HUVECs, based on the cell-free, physical binding assays (see also Fig. 1a). We applied MNP-to-virus ratios of 3–3,000 fg Fe per VP (Fig. 2a and b). All the MNPs tested showed maximal transduction efficiency at a LV/MNP ratio of 300 fg Fe per VP as demonstrated by fluorescence microscopy (Fig. 2a) and flow cytometry analysis (Fig. 2b). This ratio corresponds nicely with the LV/MNP physical binding and magnetic sedimentation assays (see also Fig. 1a). In further experiments, we have analyzed the provirus integration 48 h after transduction using quantitative Realtime PCR according to a published protocol (11) (data not shown). We have detected increasing numbers of provirus per genome with increasing LV/MNP ratios with an average provirus integration of 1 copy per genome at the ratio of 300 fg Fe/VP; this corresponds to an approximate 10 fold increase compared to virus alone (data not shown).

Next, we compared transduction efficiencies of the four MNPs in the different endothelial cell lines (Fig. 3a-d). In HUVECs, classical overnight infection (V'ON) resulted in high transgene expression and MNP-assisted LV transduction did not further improve the levels of GFP-positive cells (Fig. 3a). In the other cell lines (bPAECs, meEPCs, hlEPCs), we observed low transgene expression after overnight infection (Fig. 3b-d). Importantly, a 1.8–2.4 fold increase in transduction efficiency was achieved by binding of LVs to MNPs (Fig. 3b-d). Overall, LV/PEI-Mag combinations resulted in the highest transduction efficiency. For the two negatively charged MNPs (PALD2-Mag1 and SO-Mag5), we observed different efficiencies in the different cell types: PALD2-Mag1 was better for bPAECs and meEPCs, SO-Mag5 achieved higher transduction rates in hlEPCs. Thus, MNP-guided lentiviral transduction resulted in equal or even higher transduction efficiency compared to classical overnight transduction with PEI-Mag MNPs being the most efficient. Clear differences were observed for the same MNP in different endothelial cell types.

Additionally, we investigated the iron uptake by non-heme-iron assay in HUVECs. By comparing the iron concentration applied to the cells by LV/MNP transduction and the cellular iron measured with the assay a recovery rate can be calculated that provides information concerning the ability of the cells for the uptake of MNPs (Fig. 3e). All four MNPs exhibited a high cellular iron uptake ranging from approximately 63% to around 82% of the MNPs applied with SO-Mag5 resulting in the highest iron recovery of 81.6 ± 2.7% of the applied iron dose reflecting an efficient MNP uptake.

A crucial aspect for the use of MNPs is their potential toxicity. This was analyzed in HUVECs using two different

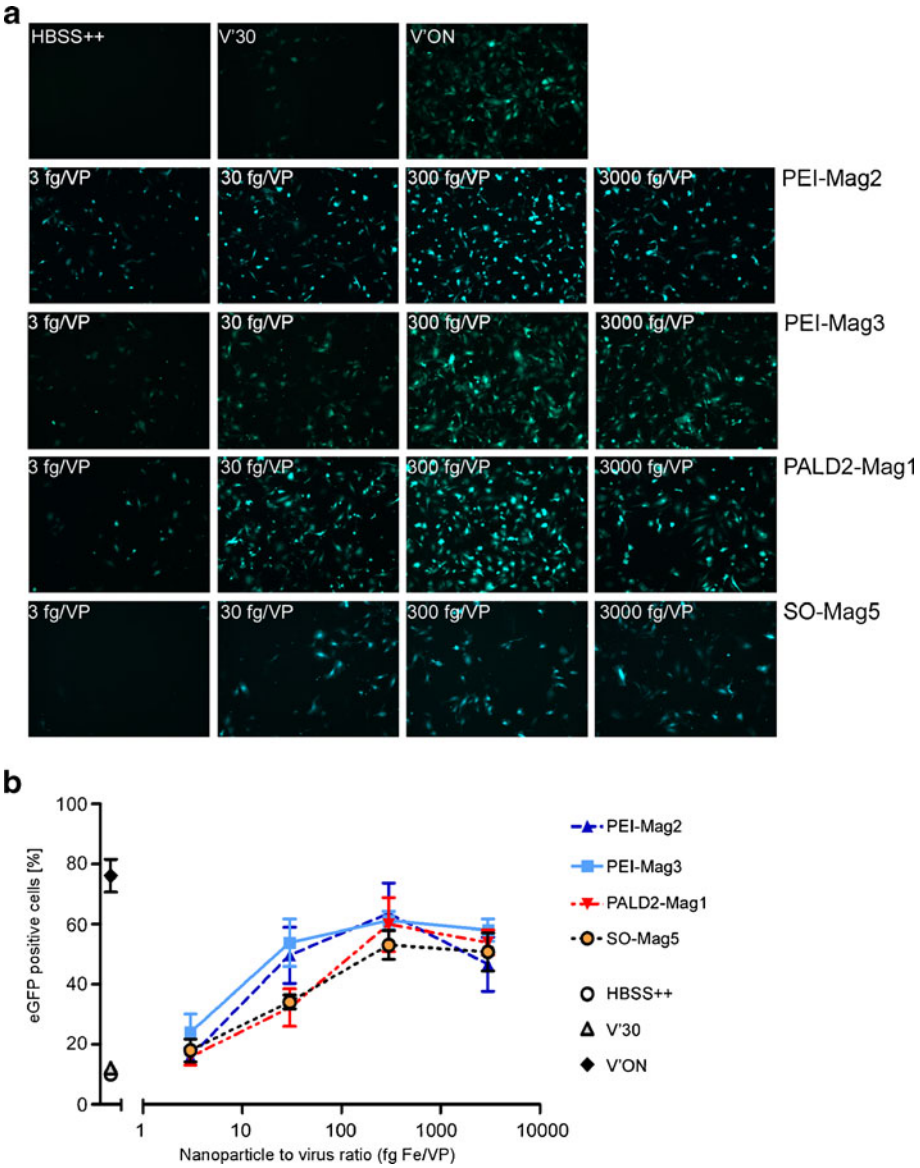

Fig. 2 Analysis of cellular transduction efficiency of LV/MNP complexes. HUVECs were transduced with LV/MNP (3 to 3,000 fg Fe per VP, MOI5) and fluorescence images were taken 48 h after transduction (**a**) or percentage of eGFP positive cells was determined via flow cytometry (**b**). Controls: buffer without LVs and MNPs (HBSS++), buffer with LV and without MNPs (V'30), LV without MNP but transduction overnight at 37°C in medium (V'ON). *Representative images of n≥3 are shown* (**a**)*; n≥3, mean±SEM* (**b**).

toxicity assays that measure either cell viability (MTT assay) or cell lysis (LDH assay). Applying LV/MNP complexes at the optimal concentration of 300 fg Fe per VP at a MOI of 5, no toxicity was detectable neither with the MTT (Fig. 3f) nor the LDH assay (Fig. 3g). Dose escalation experiments using up to 100 fold higher MNP concentrations at the same MOI revealed no toxicity for the four MNPs as measured by LDH release (Fig. 3h). Furthermore, only a slight increase of LDH was detectable at a more than 300 fold increase of the MNP concentration to 100,000 fg Fe per VP. Analysis of cell toxicity was preferentially performed at 18 h after transduction, because the MNPs are rapidly taken up by endothelial cells. We explored potential toxic effects also at a later time point (48 h) after the transduction (data not shown) and also these experiments did not reveal adverse side effects of MNP loading.

Taken together, no toxicity of the LV/MNP complexes was detectable at a moderate virus dose per cell (i.e. MOI 5) in the range of the maximal binding capacity (i.e. 300 fg Fe/VP) for the four MNPs studied.

LV/MNP Transduction Under Flow Conditions

A potential application of MNP guided local LV transduction *in vivo* requires LV/MNP complexes with a magnetic moment that is high enough to be magnetically attracted even under physiological flow stress. To analyze the magnetic responsiveness and thus, the magnetic moment of LV/MNP complexes, we measured their time-dependent optical density during application of a permanent gradient magnetic field (27) (Fig. 4a and Table I). The two PEI-Mag MNPs showed an identical low magnetophoretic mobility (ca. 0.9 μm/s) and low magnetic moment (1.0±0.1 to 1.5±0.2

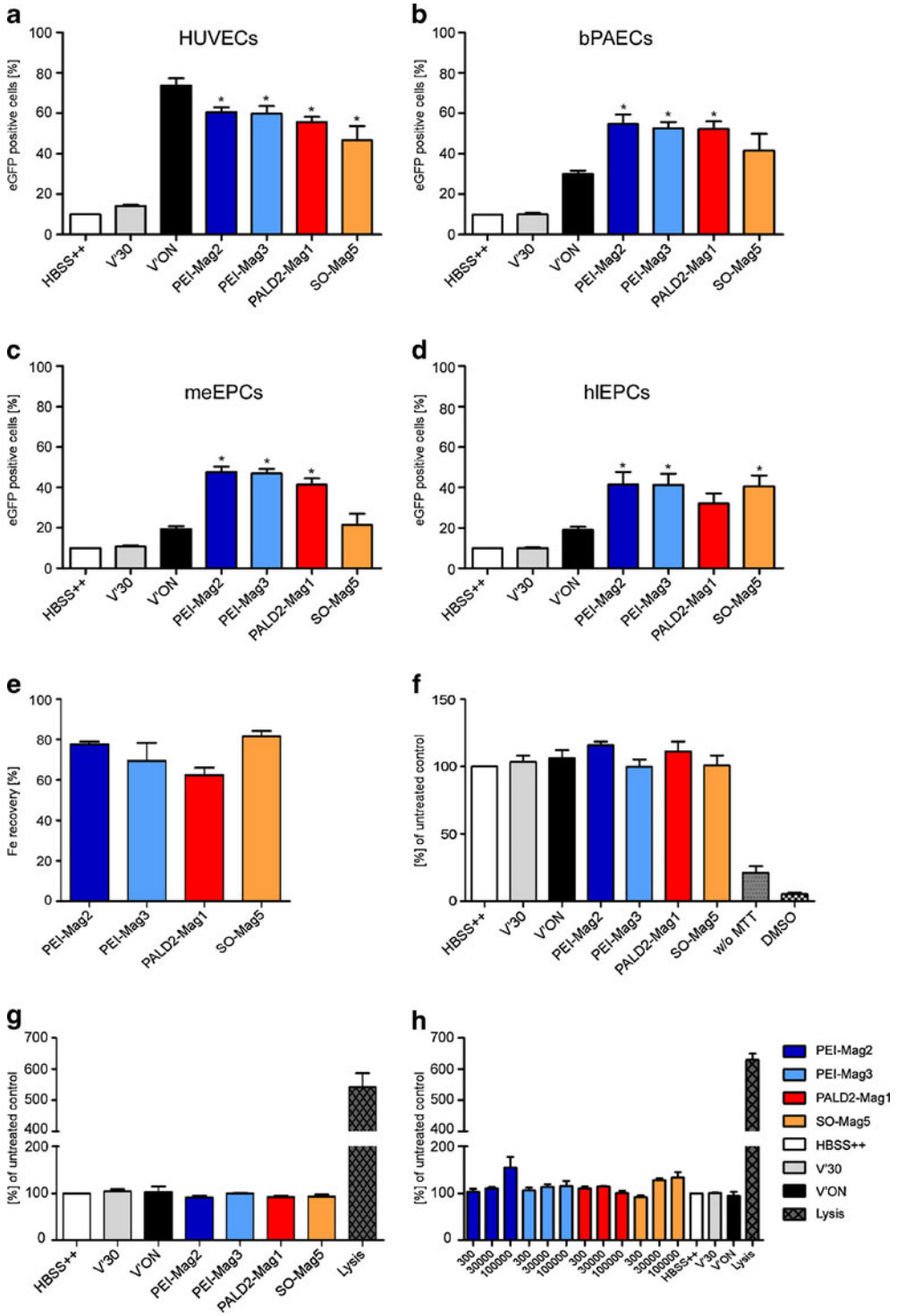

Fig. 3 Transduction efficiency and cell viability using LV/MNP complexes. (**a**-**d**) Transduction efficiency of different cell lines. Cells (HUVECs (**a**), bPAECs (**b**), meEPCs (**c**) and hlEPCs (**d**)) were transduced with LV/MNP (300 fg Fe per VP, MOI 5) and percentage of eGFP positive cells was determined via flow cytometry 48 h after transduction. *n* ≥ 3, *mean+SEM. Statistical significance compared to V'ON (calculated one-way ANOVA and post test) marked by asterisk* *, $p < 0.05$. (**e**) Cellular iron uptake of LV/MNP complexes. HUVECs were transduced with LV/MNP (300 fg Fe per VP, MOI 5). 48 h after transduction iron concentration was measured using a non-heme-iron assay and recovery was determined compared to iron (MNP) applied. *n=3, mean+SEM.* (**f**, **g**) Toxicity analysis of LV/MNP transduced cells. HUVECs were transduced with LV/MNP (300 fg Fe per VP, MOI 5). 18 h after transduction cells were analyzed using MTT-assay (**f**) or LDH-assay (**g**). Controls: buffer without LVs and MNPs (HBSS++), buffer with LV and without MNPs (V'30), LV without MNP but transduction overnight at 37°C in medium (V'ON), control without dye MTT (w/o MTT), control with complete lysed cells (DMSO, lysis). (**h**) Toxicity analysis of LV/MNP transduced cells with different MNP concentrations. HUVECs were transduced with LV/MNP (300 to 100,000 fg Fe per VP, MOI 5). 18 h after transduction cells were analyzed using LDH assay. *n* ≥ 3, *mean+SEM.*

E-15 Am²), whereas the LV/SO-Mag5 complexes exhibited the fastest magnetic sedimentation (1.9±0.4 μm/s) and thus, the highest magnetic moment (3.3±0.7 E-15 Am²). PALD2-Mag1 showed an intermediate magnetophoretic mobility (1.1±0.1 μm/s) and magnetic moment (2.2±0.2 E-15 Am²), respectively.

Next, we examined whether the magnetic moment of the different LV/MNP combinations is high enough to overcome hydrodynamic flow stress and to achieve local cell transduction in a magnetic gradient field. HUVECs were seeded in a perfusion system (Fig. 4b, *top*) and perfused with medium containing LV/MNP under physiological circulation conditions with or without a magnetic gradient field. All LV/MNP complexes exhibited a very high transduction rate in the presence of a magnetic gradient field (Fig. 4b and c) with 77.0±10.4% (LV/PEI-Mag3), 84.5±9.2% (LV/SO-Mag5), 93.3±5.2% (LV/PEI-Mag2) and 96.2±1.2% (LV/PALD2-Mag1) eGFP positive cells. This clearly demonstrates a high LV/MNP transduction efficiency under physiological flow conditions, because almost no transduction was observed in absence of the magnetic gradient field (1.3±0.6 to 2.4±0.9% eGFP positive cells). Correspondingly, almost no LV transduction was achieved without MNPs independently of the magnetic gradient field (2.7±0.7% without and 3.0±0.8% eGFP transgenic with magnets) (Fig. 4c).

Ex vivo Engraftment of LV/MNP Transduced Cells

Cell replacement is the basis for regenerative medicine and re-endothelialization of damaged vessels could be an interesting concept for the local treatment of cardiovascular diseases. Therefore, we tested whether LV/MNP transduced HUVECs can be trapped within the tunica intima of an explanted murine aorta by using an *ex vivo* flow loop system (11) upon perfusion for 30 min at a flow rate of 4 ml/min. We examined cells treated with LV/MNP complexes with one positively (PEI-Mag2) and one negatively (PALD2-Mag1) charged MNP. First, magnetic responsiveness of LV/MNP transduced cells was analyzed (Fig. 5a). Although the optimal LV/MNP ratio for transduction (300 fg Fe/VP) was used, the PEI-Mag2 and PALD2-Mag transduced cells showed only a rather low magnetic moment of 80.1±12.9 and 65.9±7.4 E-15 Am² per cell, respectively (Table II). Next, the LV/MNP transduced cells were applied in the *ex vivo* flow loop system (Fig. 5b). Neither LV/PEI-Mag2 nor LV/PALD2-Mag1 infected cells were localized at the intima of the murine vessel indicating that the magnetic moment of the cells was too low for magnetically guided local cell positioning.

To increase the magnetic moment of the transduced cells, we additionally applied SO-Mag5 to the cells before transduction resulting in 4.5–4.7 pg Fe per magnetically sedimented cell for PEI-Mag2 and PALD2-Mag1, respectively (Table I).

This MNP was chosen, because it exhibited the highest cellular iron uptake (see also Fig. 3e) and the highest magnetic moment during LV/MNP complexation (see also Fig. 4a and Table I). In comparison to LV/MNP transduced cells without addition of SO-Mag5 (see also Fig. 5a and Table II), a much faster magnetic sedimentation and thus a higher magnetic moment of the SO-Mag5 loaded cells was registered (Fig. 5c, Table II). We next tested if the magnetic moment of these labeled cells of 365.5 and 387.9 E-15 Am²/cell (Table II) is high enough to overcome shear forces in the *ex vivo* loop system (Fig. 5d). Both combinations (SO-Mag5+LV/PEI-Mag2 and SO-Mag5+LV/PALD2-Mag1) clearly showed a localized deposit of HUVECs at the intima of the murine vessel. Analysis of LV/MNP transduced and MNP loaded cells did not reveal toxicity in the LDH- and MTT assays (data not shown).

Taken together, optimization of LV/MNP assembly results in improved transduction efficiencies. However, this does not per se result in cellular magnetic moments that are high enough for positioning of transduced cells. Nevertheless, a high enough cellular magnetic moment can be achieved by loading transduced cells with additional MNPs that have a high magnetic moment.

DISCUSSION

Local gene targeting of endothelial cells would be an attractive tool for gene therapy. In addition, local cell positioning is an important concept of cell based therapies.

For achieving this goal of regional gene and cell targeting, we applied magnetically guided LVs that were associated with MNPs.

Due to their capability of being attracted in a magnetic gradient field, MNPs can be used for the localized delivery of drugs and biomolecules including DNA, RNA and proteins (33,34). In a recent publication, magnetic iron oxide particles were even employed for magnetically guided *in vitro* delivery of a malaria DNA vaccine (35). In this work PEI-coated nanoparticles resulted in efficient DNA binding and much higher transfection rates upon gradient magnetic field application were reported compared to lipofectamine mediated transfection (35). This study is another example for the broad range of potential applications of magnetic nanoparticles. Several other publications have shown that MNPs can also be used for the magnetically assisted delivery of viral vectors (36–38).

In the study presented here, we set out to improve MNP-based lentiviral gene transfer. A broad spectrum of differently charged and coated MNPs of the core shell type with a hydrodynamic diameter ranging from 20 to 500 nm was investigated. We focused on two positively charged MNPs

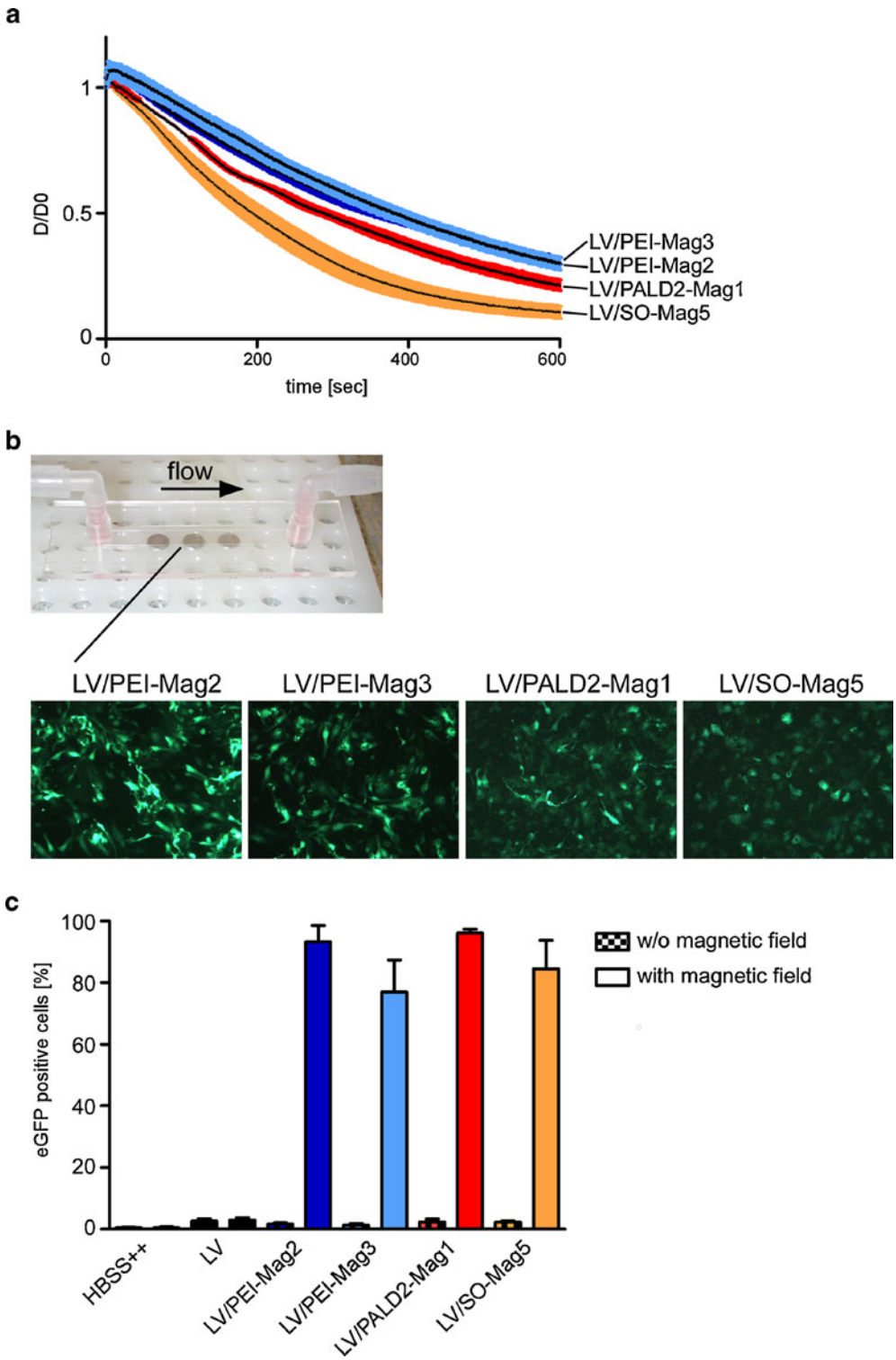

Fig. 4 Magnetic behaviour of LV/MNP complexes and transduction during perfusion. (**a**) Magnetic behavior of LV/MNP complexes. LV/MNP complexes (300 fg Fe per VP) were analyzed using magnetic responsiveness measurement (normalized; D/D0). *n=3, mean±SEM*. (**b**, **c**) Flow loop perfusion of cells with LV/MNP complexes. HUVECs were seeded in a flow chamber (**b**, *top*) and adhered cells were perfused with LV/MNP complexes in HBSS++ (300 fg Fe/VP, MOI50) for 15 min in presence (with magnetic field) or absence (w/o magnetic field) of three permanent magnets. As controls LV without MNP (LV) or buffer without LVs and MNPs (HBSS++) were used. Fluorescence images are shown after perfusion (with magnetic gradient field) (**b**, *below*). Cells were detached, expanded and analyzed using flow cytometry. *n=3, mean+SEM*. (**c**).

Table I Characteristics of the LV/MNP Complexes[a]

	LV/PEI-Mag2	LV/PEI-Mag3	LV/PALD2-Mag1	LV/SO-Mag5
elektrokinetic potential ξ (mean±SD, mV)	+11.4±0.1	+9.2±0.2	−9.9±0.05	−12.8±1.7
magnetophoretic mobility v_z (mean±SD, μm/s)[b,c]	0.9±0.1	0.9±0.01	1.1±0.1	1.9±0.4
magnetic moment M (mean±SD, 1E-15 Am^2)[b]	1.0±0.1	1.5±0.2	2.2±0.2	3.3±0.7

[a] assembling in HBSS++ (300 fg Fe/VP, final LV concentration: 1E+08 VP/ml)

[b] measured at an average magnetic field ⟨*B*⟩ of 0.213 ± 0.017 T

[c] measured at an average magnetic field gradient ⟨∇*B*⟩ of 4 ± 2 T/m

(PEI-Mag2, PEI-Mag3) and two differently coated, negatively charged particles (PALD2-Mag1 and SO-Mag5). Cell-free, physical binding assays showed maximal assembling of LV/MNP complexes at ratios between 100 to 300 fg Fe/VP for all particles analyzed. We observed lower LV/MNP ratio for half maximal binding for the positively charged MNPs indicating better binding of LVs to these MNPs as compared to the negatively charged MNPs due to direct electrostatic interaction between positively charged MNPs and negatively charged LVs. Furthermore, various

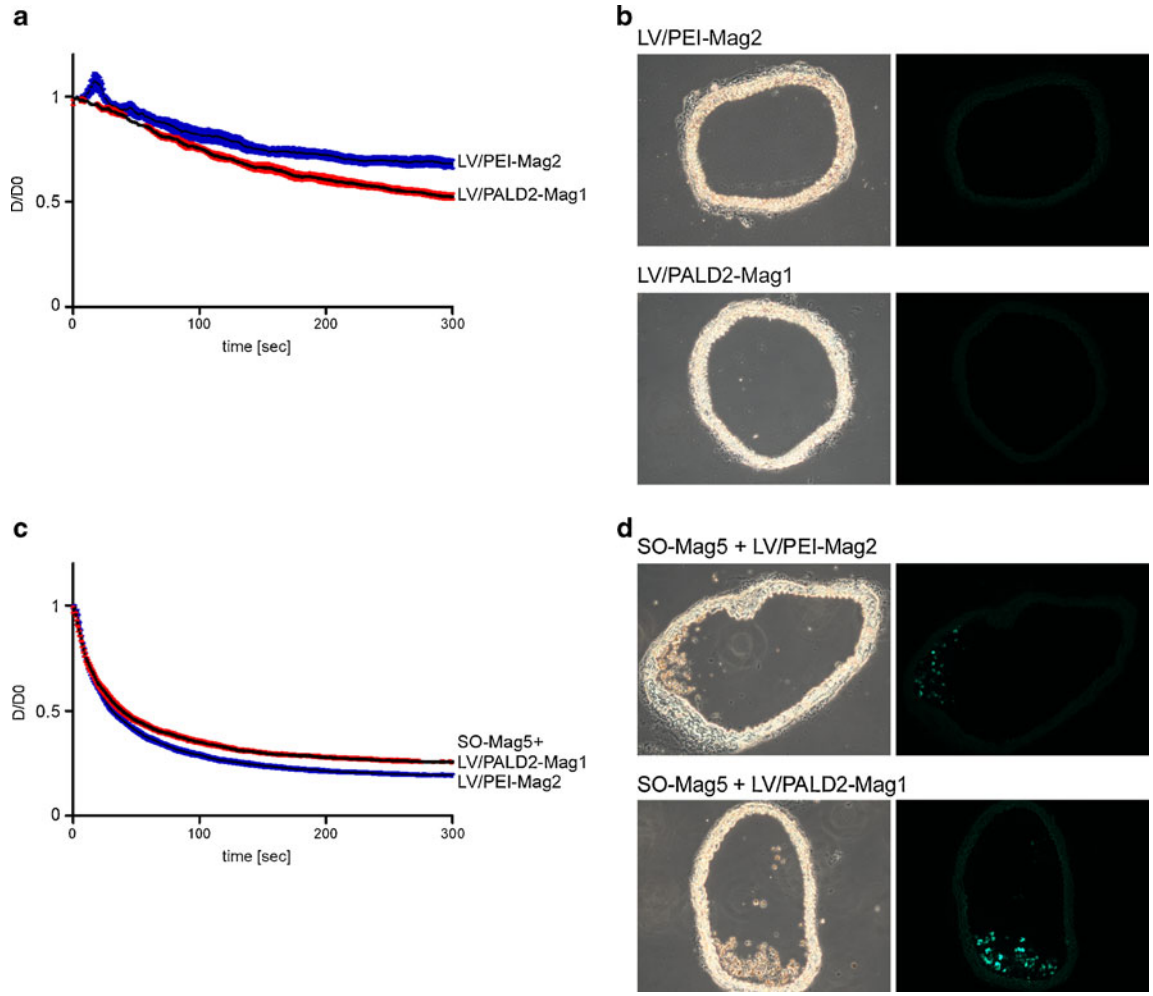

Fig. 5 Magnetic behaviour of LV/MNP transduced cells and *ex vivo* aorta perfusion. (**a**, **c**) Magnetic behavior of LV/MNP transduced cells. HUVECs were either not additionally loaded (**a**) or labeled with SO-Mag5 (**c**) and thereafter transduced with LV/MNP (300 fg Fe per VP, MOI 5) and analyzed using magnetic responsiveness measurement (normalized; D/D0). *n=3, mean±SEM*. (**b**, **d**) *Ex vivo* aorta perfusion with LV/MNP transduced cells. An explanted murine aorta was perfused for 30 min with 100,000 LV/MNP transduced HUVECs (300 fg Fe per VP, MOI 5) 48 h after transduction, that were prior to infection either not SO-Mag5 loaded (**b**) or additionally labeled with SO-Mag5 (**d**). Cryosections of the aorta are shown in brightfield (left) and as fluorescence image (right).

Table II Characteristics of LV/MNP Transduced Cells[a]

	LV/PEI-Mag2	LV/PALD2-Mag1	LV/PEI-Mag2	LV/PALD2-Mag1
addition of SO-Mag5 (100 pg applied Fe SO-Mag5/seeded cell)	–	–	+	+
magnetophoretic mobility v_z (mean±SD, μm/s)[b, c]	2.5±0.4	2.0±0.2	12.2±0.4	11.9±0.1
magnetic moment M/cell (mean±SD, 1E-15 Am²)[b]	80.1±12.9	65.9±7.4	365.5±59.9	387.9±4.2
cell associated iron (pg Fe per magnetically sedimented cell)	1.3±0.2	1.1±0.1	4.5±0.7	4.7±0.1

[a] LV/MNP transduction of HUVECs with 300 fg Fe/VP at MOI 5

[b] measured at an average magnetic field ⟨*B*⟩ of 0.213 ± 0.017T

[c] measured at an average magnetic field gradient ⟨∇*B*⟩ of 4 ± 2 T/m

publications have shown that PEI supports the complexation of silica iron oxide based MNPs to lenti- and adenoviral vectors leading to high transduction rates (39–41). The positively charged MNPs used in this study are both PEI coated and displayed overall the highest transduction efficiencies. In contrast, the negatively charged MNPs can assemble with LVs in the presence of divalent cations (29). In addition, HIV-derived lentiviral particles contain hydrophobic residues (42) that could mediate hydrophobic interactions with MNPs (e.g. PALD2-Mag1).

Another important parameter for LV/MNP complex formation is the solvent used for assembling the complexes. Interestingly, the LV/MNP interaction was stable even in the presence of serum, but only after complex formation in serum-free buffer.

Transduction efficiency of the LV/MNP complexes was studied in different endothelial cells of human, bovine and murine origin. We used two primary endothelial cells (HUVECs, bPAECs) as well as endothelial precursor cells that can develop to mature endothelial cells. Although transduction efficiencies for the four MNPs was lower than overnight transduction in HUVECs, 1.8 to 2.4 fold higher transduction efficacies were achieved for MNP transduction at non permissive conditions (4°C, 30 min) in bPAECs and meEPCs as well as hlEPCs as compared to the classical overnight infection at 37°C. The use of positively charged (PEI-coated) MNPs always resulted in high transgene expression. However, we observed different transduction levels for individual MNPs in the different cell lines. Thus, based on the analysis of one specific cell line, one cannot predict which LV/MNP combination is optimal for another cell line.

A basic requirement for MNP-guided LV gene transfer is a sufficient magnetic moment of the LV/MNP complexes within the magnetic gradient field. Although the MNPs studied exhibited a 3 fold difference in the magnetic moments of their LV complexes (1 to 3 E-15 Am²), the cell transduction experiments suggest that these magnetic moments are high enough for efficient concentration of the complexes at the cell membrane and for internalization of the exogenic iron in the cells. Importantly, the magnetic moments of the LV/MNP complexes were even high enough to overcome physiological flow conditions, and more than 70% of the cells subjected to magnetic gradient field under flow were transduced. In contrast, without magnetic gradient field or without association to MNPs almost no lentiviral transduction was observed (~2 to 3% transgenic cells).

Finally, we studied local cell positioning of magnetically labeled cells. We used the optimal LV/MNP ratio of 300 fg Fe/VP to transduce endothelial cells and applied the labeled cells for an *ex vivo* perfusion of a murine aorta. However, the cellular magnetic moment achieved with this low amount of Fe (ca. 1 pg Fe/cell) was too low to trap the cells within the tunica intima of the vessel. Therefore, we additionally treated the cells with a MNP that has a high magnetic moment to increase the magnetic moment of the transduced cells to up to almost 400 E-15 Am² per cell (nearly 5 pg Fe per cell) and achieved local cell positioning. Interestingly, bovine aortic endothelial cells loaded with polymeric MNPs and a magnetic moment of about 200 E-15 Am² per cell were already successfully targeted to steel stent wires by application of a magnetic gradient field *in vivo* (15).

Apart from MNP-assisted LV guiding also other approaches have been published for localized lentiviral mediated gene expression. Collagen hydrogels have been used to promote subcutaneous LV gene delivery *in vivo* (43). In addition, LVs can be complexed with hydroxylapatite nanoparticles to achieve increased LV retention and efficient LV delivery (43). An important aspect of MNP-based gene transfer is targeting of MNP-containing cells to tissues as well as the direct targeting of LV/MNP complexes to tissues by use of a gradient magnetic field; these approaches would also enable local gene delivery *in vivo*. Other applications employing similar techniques comprise the use of magnetic stents (44). It is also worthwhile to mention that local cell transduction under flow conditions reveals high efficiency when using LV/MNP complexes in combination with a gradient magnetic field. Thus, in the long term we envision the combination of systemic intravascular application and site specific enrichment of LV/MNP complexes for gene- and cell therapy purposes. In this study we have established important basics for such applications.

CONCLUSION

Taken together, by analyzing different parameters including binding capacity, magnetic responsiveness, transduction efficiency and cellular iron uptake, we were able to optimize LV/MNP assembly. None of the MNPs tested showed cytotoxicity as analyzed by two assays that are either based on cell metabolic activity or cell lysis. Different endothelial cell lines were tested regarding the most efficient LV/MNP combination. Importantly, in three different endothelial cell types, 1.8 to 2.4 fold higher transduction efficiencies as compared to classical overnight transduction were achieved even under non-permissive conditions (4°C, 30 min). Furthermore, high efficient local LV gene transfer in endothelial cells was possible under physiological shear stress. Additionally, magnetically labeled lentiviral transduced cells were trapped *ex vivo* under flow conditions.

ACKNOWLEDGEMENTS

For excellent technical assistance we are thankful to Christina Stichnote, Institute of Pharmacology and Toxicology, University of Bonn, Germany and Anja Wolf, Institute of Experimental Oncology and Therapy Research, Klinikum rechts der Isar der TU München. For providing human and murine EPCs we thank Ulrich Becher and Katharina Peske, Institute of Internal Medicine II, University of Bonn, Germany and Christian Kupatt, Institute of Internal Medicine I, University of Munich, Germany.

This work was supported by the German Research Foundation within the DFG Research Unit FOR917, by the North Rhine-Westphalia (NRW) International Graduate Research School BIOTECH-PHARMA and by the Ministry of Innovation, Science, Research and Technology of the State of NRW within the junior research group of Daniela Wenzel ("Magnetic nanoparticles (MNPs) - endothelial cell replacement in injured vessels").

REFERENCES

1. Pfeifer A, Verma IM. Virus vectors and their application. In: Howley PM, Knipe DM, Griffin D, Lamb RA, Martin A, Roizman B, Straus SE, editors. Fields Virology. Philadelphia: Lippincott-Raven Publishers; 2001. p. 469–91.
2. Naldini L. Lentiviruses as gene transfer agents for delivery to non-dividing cells. Curr Opin Biotechnol. 1998;9(5):457–63.
3. Trono D. Lentiviral vectors: turning a deadly foe into a therapeutic agent. Gene Ther. 2000;7(1):20–3.
4. Verma IM, Weitzman MD. Gene therapy: twenty-first century medicine. Annu Rev Biochem. 2005;74:711–38.
5. Goff SP. Retroviridae: the viruses and their replication. In: Knipe DM, Howley PM, Griffin DE, Lamb RA, Martin MA, Roizman B, Straus SE, editors. Fields virology, vol 2. 4th ed. Philadelphia: Lippincott-Raven Publishers; 2001. p. 1871–939.
6. Desrosiers RC. Nonhuman lentiviruses. In: Knipe DM, Howley PM, Griffin DE, Lamb RA, Martin MA, Roizman B, Straus SE, Straus SE, editors. Fields Virology, vol 2. 4th ed. Philadelphia: Lippincott-Raven Publishers; 2001. p. 2095–121.
7. Cavazzana-Calvo M, Payen E, Negre O, Wang G, Hehir K, Fusil F, *et al.* Transfusion independence and HMGA2 activation after gene therapy of human beta-thalassaemia. Nature. 2010;467 (7313):318–22.
8. Cartier N, Hacein-Bey-Abina S, Bartholomae CC, Veres G, Schmidt M, Kutschera I, *et al.* Hematopoietic stem cell gene therapy with a lentiviral vector in X-linked adrenoleukodystrophy. Science. 2009;326(5954):818–23.
9. Pariente N, Morizono K, Virk MS, Petrigliano FA, Reiter RE, Lieberman JR, *et al.* A novel dual-targeted lentiviral vector leads to specific transduction of prostate cancer bone metastases *in vivo* after systemic administration. Mol Ther. 2007;15(11):1973–81.
10. Scherer F, Anton M, Schillinger U, Henke J, Bergemann C, Kruger A, *et al.* Magnetofection: enhancing and targeting gene delivery by magnetic force *in vitro* and *in vivo*. Gene Ther. 2002;9(2):102–9.
11. Hofmann A, Wenzel D, Becher UM, Freitag DF, Klein AM, Eberbeck D, *et al.* Combined targeting of lentiviral vectors and positioning of transduced cells by magnetic nanoparticles. Proc Natl Acad Sci U S A. 2009;106(1):44–9.
12. Alexiou C, Arnold W, Klein RJ, Parak FG, Hulin P, Bergemann C, *et al.* Locoregional cancer treatment with magnetic drug targeting. Cancer Res. 2000;60(23):6641–8.
13. Strebhardt K, Ullrich A. Paul Ehrlich's magic bullet concept: 100 years of progress. Nat Rev Cancer. 2008;8(6):473–80.
14. Chorny M, Fishbein I, Yellen BB, Alferiev IS, Bakay M, Ganta S, *et al.* Targeting stents with local delivery of paclitaxel-loaded magnetic nanoparticles using uniform fields. Proc Natl Acad Sci U S A. 2010;107(18):8346–51.
15. Polyak B, Fishbein I, Chorny M, Alferiev I, Williams D, Yellen B, *et al.* High field gradient targeting of magnetic nanoparticle-loaded endothelial cells to the surfaces of steel stents. Proc Natl Acad Sci U S A. 2008;105(2):698–703.
16. Hatzopoulos AK, Folkman J, Vasile E, Eiselen GK, Rosenberg RD. Isolation and characterization of endothelial progenitor cells from mouse embryos. Development. 1998;125(8):1457–68.
17. Follenzi A, Ailles LE, Bakovic S, Geuna M, Naldini L. Gene transfer by lentiviral vectors is limited by nuclear translocation and rescued by HIV-1 pol sequences. Nat Genet. 2000;25(2):217–22.
18. Pfeifer A, Hofmann A. Lentiviral transgenesis. Methods Mol Biol. 2009;530:391–405.
19. Dull T, Zufferey R, Kelly M, Mandel RJ, Nguyen M, Trono D, *et al.* A third-generation lentivirus vector with a conditional packaging system. J Virol. 1998;72(11):8463–71.
20. Mykhaylyk O, Antequera YS, Vlaskou D, Plank C. Generation of magnetic nonviral gene transfer agents and magnetofection in vitro. Nat Protoc. 2007;2(10):2391–411.
21. Mykhaylyk O, Sanchez-Antequera Y, Vlaskou D, Hammerschmid E, Anton M, Zelphati O, *et al.* Liposomal magnetofection. Methods Mol Biol. 2010;605:487–525.
22. Mykhaylyk O, Vlaskou D, Tresilwised N, Pithayanukul P, Möller W, Plank C. Magnetic nanoparticle formulations for DNA and siRNA delivery. J Magn Magn Mat. 2007;311(1):275–81.
23. Sanchez-Antequera Y, Mykhaylyk O, Thalhammer S, Plank C. Gene delivery to Jurkat T cells using non-viral vectors associated with magnetic nanoparticles. Int J Biomedical Nanoscience and Nanotechnology. 2010;1(2/3/4):202–29.
24. Mykhaylyk O, Zelphati O, Hammerschmid E, Anton M, Rosenecker J, Plank C. Recent advances in magnetofection and its potential to deliver siRNAs *in vitro*. Methods Mol Biol. 2009;487:111–46.
25. Kowalski JB, Tallentire A. Substantiation of 25 kGy as a sterilization dose: a rational approach to establishing verification dose. Radiat Phys Chem. 1999;54(1):55–64.

26. Krill CE, Birringer R. Estimating grain-size distributions in nanocrystalline materials from X-ray diffraction profile analysis. Philos Mag A. 1998;77(3):621–40.
27. Mykhaylyk O, Zelphati O, Rosenecker J, Plank C. siRNA delivery by magnetofection. Curr Opin Mol Ther. 2008;10(5):493–505.
28. Mykhaylyk O, Steingotter A, Perea H, Aigner J, Botnar R, Plank C. Nucleic acid delivery to magnetically-labeled cells in a 2D array and at the luminal surface of cell culture tube and their detection by MRI. J Biomed Nanotechnol. 2009;5(6):692–706.
29. Haim H, Steiner I, Panet A. Synchronized infection of cell cultures by magnetically controlled virus. J Virol. 2005;79(1):622–5.
30. Benninghoff A, Drenckhahn D. Anatomie, Makroskopische Anatomie, Embryologie und Histologie des Menschen. 16 ed. Drenckhahn D, editor. München: Elsevier; 2004.
31. Dimitrov DS. Virus entry: molecular mechanisms and biomedical applications. Nat Rev Microbiol. 2004;2(2):109–22.
32. Tempaku A. Random Brownian motion regulates the quantity of human immunodeficiency virus type-1 (HIV-1) attachment and infection to target cell. Journal of Health Science. 2005;51(2):237–41.
33. Chomoucka J, Drbohlavova J, Huska D, Adam V, Kizek R, Hubalek J. Magnetic nanoparticles and targeted drug delivering. Pharmacological Research. 2010;62(2):144–9.
34. Shubayev VI, Pisanic Ii TR, Jin S. Magnetic nanoparticles for theragnostics. Adv Drug Deliver Rev. 2009;61(6):467–77.
35. Al-Deen FN, Ho J, Selomulya C, Ma C, Coppel R. Superparamagnetic nanoparticles for effective delivery of malaria DNA vaccine. Langmuir. 2011;27(7):3703–12.
36. Chorny M, Fishbein I, Alferiev I, Levy RJ. Magnetically responsive biodegradable nanoparticles enhance adenoviral gene transfer in cultured smooth muscle and endothelial cells. Mol Pharm. 2009;6(5):1380–7.
37. Mykhaylyk O, Sanchez-Antequera Y, Tresilwised N, Doblinger M, Thalhammer S, Holm PS, *et al.* Engineering magnetic nanoparticles and formulations for gene delivery. J Control Release. 2011;148(1):e63–4.
38. Plank C, Scherer F, Schillinger U, Bergemann C, Anton M. Magnetofection: enhancing and targeting gene delivery with superparamagnetic nanoparticles and magnetic fields. J Liposome Res. 2003;13(1):29–32.
39. Anton M, Wolf A, Mykhaylyk O, Koch C, Gansbacher B, Plank C. Optimizing Adenoviral transduction of endothelial cells under flow conditions. Pharm Res. 2011. doi:10.1007/s11095-011-0631-2.
40. Sanchez-Antequera Y, Mykhaylyk O, van Til NP, Cengizeroglu A, de Jong JH, Huston MW, *et al.* Magselectofection: an integrated method of nanomagnetic separation and genetic modification of target cells. Blood. 2011;117(16):e171–81.
41. Tresilwised N, Pithayanukul P, Holm PS, Schillinger U, Plank C, Mykhaylyk O. Effects of nanoparticle coatings on the activity of oncolytic adenovirus-magnetic nanoparticle complexes. Biomaterials. 2011;33:256–69.
42. Agopian K, Wei BL, Garcia JV, Gabuzda D. A hydrophobic binding surface on the human immunodeficiency virus type 1 Nef core is critical for association with p21-activated kinase 2. J Virol. 2006;80(6):3050–61.
43. Shin S, Shea LD. Lentivirus immobilization to nanoparticles for enhanced and localized delivery from hydrogels. Mol Ther. Apr;18(4):700-6.
44. Rathel T, Mannell H, Pircher J, Gleich B, Pohl U, Krötz F. Magnetic stents retain nanoparticle-bound antirestenotic drugs transported by lipid microbubbles. Pharm Res. 2011. doi:10.1007/s11095-011-0643-y.